Microbiological Research 218 (2019) 66–75

Contents lists available at ScienceDirect

Microbiological Research

journal homepage: www.elsevier.com/locate/micres

Environmental conditions shape the biofilm of the Antarctic bacterium *Pseudoalteromonas haloplanktis* TAC125

Annarita Ricciardelli[a], Angela Casillo[a], Alessandro Vergara[a,b], Nicole Balasco[c], Maria Michela Corsaro[a], Maria Luisa Tutino[a], Ermenegilda Parrilli[a,*]

[a] Department of Chemical Sciences, University of Naples "Federico II", Complesso Universitario Monte Sant'Angelo, Via Cintia 4, 80126 Naples, Italy
[b] CEINGE srl, Naples, Italy
[c] Institute of Biostructures and Bioimaging, C.N.R., Naples I-80134, Italy

ARTICLE INFO

Keywords:
P.haloplanktis TAC125
Biofilm matrix
Cellulose
Low temperature
Raman microspectroscopy
Confocal laser scanning microscopy

ABSTRACT

Biofilms are the most widely distributed and successful microbial modes of life. The capacity of bacteria to colonize surfaces provides stability in the growth environment, allows the capturing of nutrients and affords protection from a range of environmental challenges and stress. Bacteria living in cold environments, like Antarctica, can be found as biofilms, even though the mechanisms of how this lifestyle is related to their environmental adaptation have been poorly investigated. In this paper, the biofilm of *Pseudoalteromonas haloplanktis* TAC125, one of the model organisms of cold-adapted bacteria, has been characterized in terms of biofilm typology and matrix composition. The characterization was performed on biofilms produced by the bacterium in response to different nutrient abundance and temperatures; in particular, this is the first report describing the structure of a biofilm formed at 0 °C. The results reported demonstrate that *Ph*TAC125 produces biofilms in different amount and endowed with different physico-chemical properties, like hydrophobicity and roughness, by modulating the relative amount of the different macromolecules present in the biofilm matrix. The capability of *Ph*TAC125 to adopt different biofilm structures in response to environment changes appears to be an interesting adaptation strategy and gives the first hints about the biofilm formation in cold environments.

1. Introduction

Bacteria in nature are most often found associated with surfaces in communities known as biofilms (Hall-Stoodley et al., 2004). Biofilm has been defined as an aggregate of microorganisms in which the cells are surrounded by a self-produced matrix constituted of extracellular polymeric substances (EPS) and adhere to each other and/or to a surface. The intermolecular interactions between the EPS molecules determine the mechanical properties of the matrix, and the physiological activity of the organisms in the biofilm (Flemming and Wingender, 2010). Although the precise chemical and physical composition of the EPS varies according to the species and the growth conditions, the main biofilm matrix building blocks are bacterial proteins, extracellular DNA (eDNA) (Whitchurch et al., 2002), lipids and polysaccharides (Flemming and Wingender, 2010). The eDNA is a critical component of the biofilm matrix of several bacteria (Whitchurch et al., 2002; Seper et al., 2011), and its amount in the biofilms varies greatly from strain to strain. It has multiple functions in biofilm formation (Okshevsky et al., 2015) and influences the three-dimensional biofilm architecture and stability by acting as a cell-cell interaction polymer (Allesen-Holm et al., 2006).

The importance of proteins in the biofilm structure and function is increasingly being recognized. Matrix proteins include not only the outer membrane proteins and the secreted proteins, but also particular classes of proteins, such as the adhesins, or motility organelles, such as curli or type IV pili proteins (Flemming and Wingender, 2010; Johnson et al., 2014).

Extracellular polysaccharides are important structural components of the biofilm matrix. Most of the exopolysaccharides of the matrix are very long, with a molecular weight range of 500–2000 kDa; they can be homopolymers, such as cellulose, curdlan, and dextran, or heteropolymers, such as alginate, emulsan, gellan, and xanthan (Yildiz et al., 2014).

Biofilm architectures are highly variable, ranging from open structures, containing channels and columns of bacteria, to structures with no obvious pores and densely packed regions of cells (Wimpenny et al., 2000; Doghri et al., 2015). To date, most attention has been focused on biofilms arising from the colonization of solid-liquid (S–L) interfaces

* Corresponding author.
E-mail address: erparril@unina.it (E. Parrilli).

https://doi.org/10.1016/j.micres.2018.09.010
Received 27 July 2018; Received in revised form 24 September 2018; Accepted 28 September 2018
Available online 06 October 2018
0944-5013/

(i.e. submerged biofilms), but several other kinds of interface, as the air-liquid (A–L), also provide ecological opportunities for bacterial colonization. The biofilms formed on the surface of static liquids are usually referred to as pellicles or floating biofilms (Wimpenny et al., 2000).

Irrespective of the interface where the bacteria aggregate, the biofilm formation consists of several stages and involves numerous conserved and/or species-specific factors (Hall-Stoodley et al., 2004). In any case, the biofilm formation can be described as a developmental process with distinct stages: an 'initial adhesion', in which the microorganisms adhere to biotic or abiotic surfaces; an 'early biofilm formation', during which the microorganisms begin to produce extracellular polymeric substances (EPS); a 'biofilm maturation', involving the development of three-dimensional structures where the EPS component provides a multifunctional and protective scaffold; and finally a 'dispersal', whereby the cells leave the biofilm to reenter the planktonic phase (Sauer et al., 2002). This is a dynamic and complex process and requires a considerable energetic cost (Saville et al., 2011); however, this cost may be evolutionarily acceptable due to the structural and physico-chemical advantages deriving from the biofilm formation. First, the capacity to colonize a surface provides a high level of stability in the growth environment. Secondly, the matrix enables the biofilm to capture resources such as the nutrients that are present in the environment or that are associated with the substratum on which the biofilm is growing (Flemming and Wingender, 2010). Thirdly, the biofilm formation affords protection from a wide range of environmental challenges (Flemming et al., 2016). Moreover, the spatial organization of the cells in biofilms allows a high degree of biodiversity and complex, dynamic and synergistic interactions, including cell-to-cell communication and enhanced horizontal gene transfer (Flemming et al., 2016). Therefore, the ability to form biofilm is a selective advantage for bacteria.

Correspondingly, bacteria living in extreme environments, like Antarctica, can be found as biofilms and this ability is believed to aid their adaptation and survival in the environment (Liao et al., 2016). The capability of cold-adapted bacteria to live and proliferate at low temperatures is the result of a wide range of adaptive features (Margesin and Feller, 2010; Carillo et al., 2015; Casillo et al., 2017) but how and if the capability to form biofilm can be included into these features is poorly investigated (Smith et al., 2016; Liao et al., 2016).

In this paper, our attention has been focused on the biofilm structure of *Pseudoalteromonas haloplanktis* TAC125 (*Ph*TAC125) (Médigue et al., 2005). *Pseudoalteromonas* strains played a significant role in marine ecosystems and they have been frequently isolated from natural biofilms or surfaces of eukaryote (Holmström and Kjelleberg, 1999). They are also known to produce a wide array of compounds with pharmaceutical and antifouling potential (Isnansetyo and Kamei, 2003; Klein et al., 2011). Moreover, *Ph*TAC125 is one of the model organisms of cold-adaptation and is one of the most intensively investigated psychrophilic bacteria. The increasing interest in *Ph*TAC125 has led to the accumulation of different data types for this bacterium in the last few years, including its complete genome sequence (Médigue et al., 2005), its proteome (Piette et al., 2011), its growth phenotypes description in different conditions (Giuliani et al., 2011; Sannino et al., 2017; Wilmes et al., 2010) and the construction of a genome-scale metabolic model (Fondi et al., 2015).

The main aim of this paper was the characterization of *Ph*TAC125 biofilm in different environmental conditions to asses if and how the *Ph*TAC125 biofilm structure is shaped by the environment. In detail, the response to different temperatures (15 °C vs 0 °C) and nutrient abundance (rich medium vs synthetic medium) has been analyzed. The *Ph*TAC125 biofilm has been characterized in terms of biofilm typology and matrix composition by means of several classic experimental approaches, such as confocal laser scanning microscopy, and Raman Microspectroscopy a technique recently used to provide molecular details of the chemical composition of bacterial biofilms (Carey et al., 2017; Henry et al., 2017; Takahashi et al., 2017).

2. Materials and methods

2.1. Bacterial strains and culture conditions

Pseudoalteromonas haloplanktis TAC125 was isolated in 1992 from an Antarctic coastal seawater sample collected near the French Antarctic station Dumont d'Urville, Terre Adélie (66°40′ S; 140° 01′ E). It was grown in Brain Heart Infusion broth (BHI, Oxoid, UK) and the synthetic medium GG (10 g/L D-Gluconic acid sodium, 10 g/L glutamic acid, SCHATZ salt mixture) (Sannino et al., 2017). The biofilm formation was assessed in the static condition in the BHI medium and GG medium at 15 °C and 0 °C at different times (24 h, 48 h, 72 h, and 96 h).

2.2. Biofilm formation and assays

The quantification of the *in vitro* biofilm production was based on the method described by Christensen with slight modifications (Christensen et al., 1985). Briefly, the wells of a sterile 24-well flat-bottomed polystyrene plate were filled with 1 mL of a medium with a suitable dilution of the Antarctic bacterial culture in the exponential growth phase (about 0.1 OD 600 nm). The plates were incubated at 15 °C and 0 °C for different times (24 h, 48 h, 72 h, and 96 h). After rinsing with PBS, the adherent cells were stained with 0.1% (w/v) crystal violet, rinsed twice with double-distilled water, and thoroughly dried. To analyze the typology of the biofilm formed at the different tested conditions, the stained biofilms were photographed by a camera from the top (the submerged biofilms) and from the front (the pellicles) of the plates. Subsequently, the dye bound to the adherent cells was solubilized with 20% (v/v) acetone and 80% (v/v) ethanol. After 10 min of incubation at room temperature, the OD 590 nm was measured to quantify the total biomass of biofilm formed in each well; the OD590 values reported was obtained by subtracting the OD590 value of the control obtained in absence of bacteria. Each data point was composed of six independent samples.

2.3. Biofilm recovery

Pellicles. The biofilm formation assay was performed in BHI medium and GG medium at 15 °C, since in these conditions the biofilm formation occurred at the air-liquid interface. Briefly, the wells of a sterile 24-well flat-bottomed polystyrene plate were filled with 1 mL of a medium with a suitable dilution of a *Ph*TAC125 culture in the exponential growth phase (about 0.1 OD600 nm). Plates were incubated at 15 °C for 96 h to allow the formation of compact and resistant pellicles at the air-liquid interface. After incubation, the pellicles were recovered using a pipette and stored at −20 °C. The samples were freeze-dried for further analysis.

Submerged biofilm. The biofilm formation assay was performed in the GG medium at 0 °C, since in this condition the biofilm formation occurred at the solid-liquid interface. Briefly, sterile plastic Petri dishes (90 × 15 mm) were filled with 25 mL of the GG medium with a suitable dilution of a *Ph*TAC125 culture in the exponential growth phase (about 0.1 OD 600 nm). The plates were incubated at 0 °C for 48 h to allow a strong biofilm formation at the solid-liquid interface on the bottom of the plates. After incubation, the supernatant and the cells were discarded, and the plates were rinsed twice with filter-sterilized PBS. The submerged biofilm was recovered by scraping with a sterile cell scraper, centrifuged to remove the supernatant and stored at −20 °C. The samples were freeze-dried for further analysis.

2.4. Microbial adhesion to hydrocarbons (MATH) assay

Solution chemistry and cleaning procedure. Analytical reagent grade chemicals were used throughout and Milli-Q deionized (DI) water was used to prepare all the solutions. The electrolyte solutions were prepared with 200 mM NaCl. All the experiments were performed at

room temperature (20 ± 1 °C). The cleaning procedure for the glassware was rinsed with acetone, washing with DI water, acid-washing with 12 M HCl and finally rinsing repeatedly with DI water.

Preparation of bacteria. The *Ph*TAC125 biofilm formation was performed in the BHI medium and GG medium at 15 °C. After 96 h incubation, the biofilms (pellicles) were recovered, separated from the supernatant by centrifugation and then resuspended in a 0.2 M NaCl electrolyte solution. To remove traces of the growth medium, the biofilms were centrifuged and resuspended in a fresh electrolyte solution three times to obtain a final bacterial suspension suitable for use.

Hydrocarbons. Three different hydrocarbons were chosen: *n*-hexadecane (97–99%, Sigma), *n*-dodecane (≥ 99%, Sigma), and toluene (99.8%, Sigma). The partition coefficients were: *n*-hexadecane, log Kow = 8.20; *n*-dodecane, log Kow = 6.10; and toluene, log Kow = 2.73.

MATH assay. The cell surface hydrophobicity (CSH) of the biofilms (pellicles), recovered in the BHI medium and GG medium as previously described, was determined through the Microbial Adhesion to Hydrocarbons (MATH) assay, as a measure of their hydrophobic adherence, by following the method of (Rosenberg et al., 1980) with slight modifications. The bacterial suspension was adjusted to an absorbance (A0) of 0.6 at 600 nm. In a clean borosilicate round-bottom glass tube (16 × 150 mm), 1 mL of the test hydrocarbon was added to 4 mL of the bacterial suspension. The tube was vortexed for 2 min and set aside to rest for 30 min to allow for the phase separation. Next, a sample of the bacterial suspension was retrieved with a clean Pasteur pipette, with great care taken to avoid allowing the hydrocarbon layer to enter the pipette. The sample was then transferred to a cuvette for the final absorbance measurement (Af) at 600 nm. The adhesion of the bacteria to the hydrocarbons was evaluated as the fraction partitioned in the hydrocarbon phase, FPC. This was calculated as (FPC = 1 − Af /A0).

2.5. Motility assay

For the swarming motility assay, BHI and GG soft agar plates (0.3% agar) were used. An appropriate volume of a saturated cell culture (about 50 µL) of *Ph*TAC125, grown in the BHI medium and GG medium, was spotted on autoclaved circular pieces of Whatman Filter Paper with an average diameter of approx. 1.5 cm. Once the cells had been absorbed, the filters were placed in the center of the BHI and GG soft-agar plates and then the plates were incubated at 15 °C and at 0 °C, in parallel. To evaluate the ability of *Ph*TAC125 to swarm into a semi-solid medium, the cell spots were measured every 24 h in terms of distance from the filter. In this work, the motility is expressed as the length of the path per unit of time (mm/h).

2.6. Mannose effect on the biofilm formation

To test whether the presence of mannose affects the ability of *Ph*TAC125 to form a biofilm, a static biofilm formation assay was performed in the GG medium for 24 h at 0 °C in the presence of mannose. In detail, 200 µL of the medium with a suitable dilution of a *Ph*TAC125 culture in the exponential growth phase (about 0.1 OD 600 nm) were added into each well of a sterile 96-well flat-bottomed polystyrene plate in the absence and presence of 200 mM D-mannose (Merck KGaA) and 200 mM D-galactose (VWR International) as a control. After the incubation, the biofilm quantification was performed by means of the crystal violet method, as previously described.

2.7. Confocal laser scanning microscopy

For the confocal microscopy analysis, the biofilm formation was performed on Nunc™ Lab-Tek® 8-well Chamber Slides (n° 177445; Thermo Scientific, Ottawa, ON, Canada) in the BHI medium and GG medium at 15 °C and 0 °C for 24 h. All the microscopic observations and image acquisitions were performed with a confocal laser scanning microscope (CLSM) (LSM700-Zeiss, Germany) equipped with an Ar laser (488 nm), and a He-Ne laser (555 nm).

Bacterial Viability and Biofilm Thickness Determination. The biofilm cell viability was determined by the FilmTracer™ LIVE/DEAD® Biofilm Viability Kit (Molecular Probes, Invitrogen) following the manufacturer's instructions. Briefly, 300 µL of the medium with a suitable dilution of a *Ph*TAC125 culture in the exponential growth phase (about 0.1 OD 600 nm) were added to each well of a sterile Chamber Slide. After 24 h incubation, the plates were rinsed with filter-sterilized PBS. Then each well of the chamber slide was filled with 300 µL of a working solution of fluorescent stains, containing the SYTO® 9 green fluorescent nucleic acid stain (10 µM) and Propidium iodide, the red-fluorescent nucleic acid stain (60 µM), and incubated for 20–30 min. at room temperature, protected from light. All the excess staining was removed by rinsing gently with filter-sterilized PBS. The images were obtained using a 20X/0.8 objective. The excitation/emission maxima for these dyes are approximately 480/500 nm for the SYTO® 9 stain and 490/635 nm for propidium iodide. Z-stacks were obtained by driving the microscope to a point just out of focus on both the top and bottom of the biofilms. The images were recorded as a series of. tif files with a file-depth of 16 bits. The COMSTAT software package(Heydorn et al., 2000) was used to determine the biovolume ($\mu m^3/\mu m^2$), mean thickness (µm) and roughness coefficient (Ra*). Biovolume was defined as the number of biomass pixels in all images of a stack, multiplied by the voxel size and divided by the substratum area of the image stack. Biovolume represents the overall volume of the biofilm, and also provides an estimate of the biomass in the biofilm. Average thickness of biofilm provided a measure of the space size of the biofilm and is the most common variable in biofilm literature. Roughness coefficient is calculated from the thickness distribution of the biofilm and provides a measure of how much the thickness of the biofilm varies and is an indicator of biofilm heterogeneity. For each condition, two independent biofilm samples were used and at least two Z-stacks were performed.

2.8. Raman microspectroscopy

Raman is a technique appropriate for the investigation of biopolymer compositions in media containing high concentrations, such as in biopolymer crystals (Vergara et al., 2013, 2005) or cells. Indeed, biofilm media and substrates have been investigated by Raman microspectroscopy in order to describe the chemical composition of bacterial biofilms (Henry et al., 2017; Carey et al., 2017). A confocal Raman microscope (Jasco, NRS-3100) was used to obtain the Raman spectra. The 514 nm line of an air-cooled Ar^+ laser (Melles Griot, 35 LAP431 220) was injected into an integrated Olympus microscope and focused to a spot diameter of approximately 1 µm by a 100x objective with a final 6 mW power at the sample. A holographic notch filter was used to reject the excitation laser line. The Raman backscattering was collected using a diffraction lattice of 1200 grooves/mm and 0.1 mm slits. Typically, it took 60 s to collect a complete data set by means of a Peltier-cooled 1024 × 128 pixel CCD photon detector (Andor DU401BVI). The Raman measurements were at least triplicated for reasons of reproducibility for each spot sampled. The wavelength calibration was performed by using cyclohexane as standard.

2.9. DOC-PAGE

PAGE was performed using the system of Laemmli (Laemmli, 1970) with sodium deoxycholate (DOC) as the detergent. The separating gel contained final concentrations of 14% acrylamide, 0.1% DOC, and 375 mM Tris/HCl (pH 8.8); the stacking gel contained 4% acrylamide, 0.1% DOC, and 125 mM Tris/HCl (pH 6.8). The biofilm samples were prepared at a concentration of 0.05% in the sample buffer (2% DOC and 60 mM Tris/HCl [pH 6.8], 25% glycerol, 14.4 mM 2-mercaptoethanol, and 0.1% bromophenol blue). All the concentrations are expressed as the mass/vol percentage. The electrode buffer was composed of SDS

(1 g/L), glycine (14.4 g/L), and Tris (3.0 g/L). The electrophoresis was performed at a constant amperage of 30 mA. The gels were fixed in an aqueous solution of 40% ethanol and 5% acetic acid. The biofilm sample bands were visualized by silver staining as previously described (Tsai and Frasch, 1982).

2.10. Sugar analysis

The glycosyl analysis was performed as already reported (Carillo et al., 2014). Briefly, biofilm samples (0.5 mg) were mixed with 1 mL of HCl/CH_3OH, subjected to methanolysis for 16 h at 80 °C and then acetylated. Fatty acids were extracted twice with hexane and the methanol layer was dried and acetylated. Both the acetylated methyl glycosides and methyl esters of the fatty acids were injected into the GC–MS. All the sample derivatives were analyzed on an Agilent Technologies gas chromatograph 6850 A equipped with a mass selective detector 5973 N and a Zebron ZB-5 capillary column (Phenomenex, 30 m × 0.25 mm i.d., flow rate 1 mL/min, He as carrier gas). The acetylated methyl glycosides were analyzed using the following temperature program: 140 °C for 3 min, and 140 °C → 240 °C at 3 °C/min. The acetylated alditols were analyzed using the following temperature program: 150 °C for 3 min, and 150 °C → 330 °C at 3 °C/min.

2.11. Calcofluor binding assay

The cellulose production was detected by growing bacteria on GG or BHI agar supplemented with 200 μg/ml Calcofluor (Sigma, Milan). The plates were incubated at 0 °C or 15 C for 96 h. The colonies were visualized under a 366 nm light source.

2.12. Cellulase assay

20 mg of each sample was incubated with 0.4 mL of acetic acid 0.05 M, 0.1 mL of water, and 0.1 mL of cellulase from *Trichoderma reesei* ATCC 26921, at 37 °C for 2 h. The reaction was quenched by transferring the tube into an ice bath and centrifuged at 4 °C, 3000 rpm, 10 min. The supernatant was freeze-dried and analyzed as acetylated alditols, as reported (Pieretti et al., 2010).

2.13. DNase I and proteinase K treatment on biofilm formation

To understand if DNase I and proteinase K are able to affect the *Ph*TAC125 biofilm formation process, a static biofilm assay was performed in the presence of DNase I or proteinase K. The biofilm formation was assessed in the BHI medium and GG medium at 15 °C and 0 °C for 24 h. In detail, 200 μL of the medium with a suitable dilution of a *Ph*TAC125 culture in the exponential growth phase (about 0.1 OD 600 nm) were added into each well of a sterile 96-well flat-bottomed polystyrene plate in the absence and presence of DNase I or proteinase K at 100 μL/mL. After incubation, biofilm quantification was performed by means of the crystal violet method, as previously described (Christensen et al., 1985).

3. Results

3.1. Characterization of PhTAC125 biofilm obtained in different culture conditions

To investigate the capability of *Ph*TAC125 to form biofilm at different growth temperatures, the bacterium was grown in BHI, a rich culture medium, or in GG, a synthetic minimum medium, at 15 °C and 0 °C in static conditions, and the biofilm was evaluated at different incubation times. As shown in Fig. 1, the Antarctic bacterium was able to form biofilm in all the tested conditions and the amount of the biofilm formed in the diverse conditions was different (statistically significative shown Table S1); in the synthetic medium GG, the amount of biofilm produced by the bacterium was higher than that produced in the rich medium BHI both at 15 °C and at 0 °C (Fig. 1). Moreover, the kinetics of the biofilm formation proved to be slightly different in the analyzed conditions, considering that, at 15 °C in GG the amount of biofilm increased over time while at 0 °C decreased (Fig. 1), suggesting that the temperature strongly influences the kinetics of the biofilm formation.

Furthermore, as shown in Fig. 1 the *Ph*TAC125 biofilm accumulated mainly at the air-liquid interface forming pellicles at 15 °C in both BHI and GG media and at 0 °C only in BHI, while, interestingly, it formed biofilm mainly at the solid-liquid interface at 0 °C in the GG medium.

3.2. MATH assay on pellicles obtained in different culture conditions

The macroscopic inspection of the pellicles deriving from A–L biofilms obtained when *Ph*TAC125 was grown in BHI or GG medium was suggestive of changes in their respective structural features. In fact, pellicles from the bacterial growth in BHI medium at 15 °C after 96 h incubation proved to be stickier and slimier than those obtained in the GG in the same conditions, which, in contrast, presented more compact. Therefore, the microbial adhesion to hydrocarbons (MATH) assay was performed to assess the hydrophobicity of the *Ph*TAC125 pellicles by examining their solubility in three different solvents: toluene, *n*-dodecane, and *n*-hexadecane. As shown in Fig. 2, the *Ph*TAC125 pellicles obtained in GG medium exhibited a significant degree of solubility in all the hydrocarbon solvents examined. In contrast, the *Ph*TAC125 pellicles formed in BHI medium demonstrated negative partitioning fractions in the tested solvents, indicating that the *Ph*TAC125 GG-grown pellicles exhibited a higher hydrophobicity with respect to the *Ph*TAC125 BHI-grown ones.

3.3. Motility assay in different culture conditions

The different motility of the *Ph*TAC125 cells in the four studied conditions was evaluated (Table 1) by means of an LB soft agar motility assay (Liu et al., 2010) and was expressed as the length of the path travelled on the BHI and GG soft-agar plates per unit of time. The reduction of the flagellar motility at low temperatures has previously been reported (De Maayer et al., 2014), and indeed, as expected, at 0 °C the bacterium displayed a lower ability to move in a semi-solid medium than at 15 °C.

3.4. CLSM analysis of biofilm obtained in different culture conditions

The biofilms produced by *Ph*TAC125 in the diverse conditions were further investigated by confocal laser scanning microscopy (CLSM) to analyze the biofilm structure and the biomass distribution by means of three-dimensional biofilm images. Live/dead staining was used to visualize the *Ph*TAC125 cells encapsulated in the biofilm matrix (Figs. 3a and S1) (green indicates viable cells and red indicates damaged cells). Although the four images were clearly different, it is difficult to obtain detailed and accurate descriptions of the differences among the four biofilms, based on visual inspection only. Therefore, all the CLSM image stack data were further analyzed using the COMSTAT image analysis software package (Heydorn et al., 2000) to evaluate the different variables describing the biofilm structure. As expected, the values of the biomass and the average thickness of the biofilm obtained in the rich medium BHI were significantly lower if compared to those of the biofilm produced by *Ph*TAC125 in the GG medium at the same temperature (Fig. 3b). The analysis revealed that in the GG medium the biofilm proved to be more compact, both at 15 °C and at 0 °C, as indicated by a lower roughness coefficient (Fig. 3b). This dimensionless factor provides a measure of how much the thickness of a biofilm varies, and it is thus used as a direct indicator of biofilm heterogeneity, suggesting that the medium composition has a key role in the definition of this characteristic of the biofilm structure (Toyofuku et al., 2016; Bester et al.,

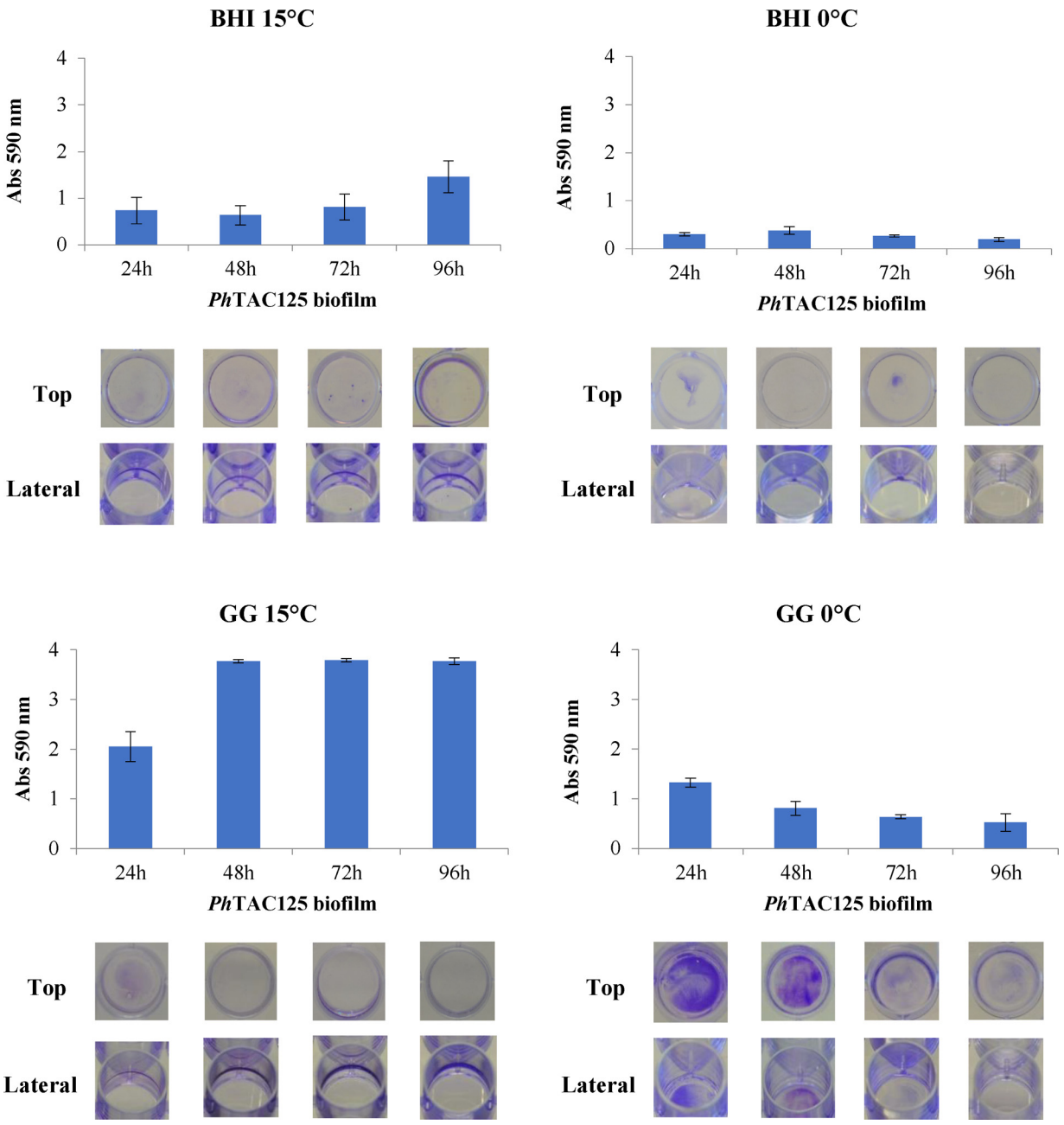

Fig. 1. Analysis of the effect of temperature and growth medium on the *Ph*TAC125 biofilm formation at different times. *Ph*TAC125 biofilm obtained at 15 °C or 0 °C in the BHI medium or in the GG medium. The biofilms were analyzed at 24 h, 48 h, 72 h, and 96 h with the crystal violet assay. Each data point was composed of six independent samples. (Top) Stained biofilms: the top view of wells allows a better vision of the submerged biofilms at the solid/liquid interface, (Lateral) whereas the lateral view is more useful to see the biofilms at the air/liquid interface.

2011; Shrout et al., 2006).

3.5. Raman microspectroscopy of PhTAC125 biofilms

High-quality Raman spectra were collected for biofilms grown at 0 °C in the GG and BHI media (spectra a and b in Fig. 4). Eventual signals coming from growth medium and/or the polystyrene supports were explored by recording the Raman spectra of the uninoculated media and of polystyrene, from which the GG-grown biofilm at 0 °C was scraped. As shown in Fig. 4, the GG medium presented several Raman bands in the 800-1500 cm^{-1} region (spectrum c in Fig. 4) that can be mainly assigned to carbohydrate-related vibrations. BHI medium was instead not active at Raman analysis (spectrum d in Fig. 4). The observed Raman bands recorded in the reference experiments were taken into consideration and not mentioned during the following analysis of microbial biofilms.

Both biofilms grown at 0 °C in the GG and BHI media showed Raman bands assignable to proteins, nucleic acids, and carbohydrates (Henry et al., 2017; Carey et al., 2017). The visual inspection of the obtained Raman spectra indicated that they were significantly different. Therefore, these spectral changes do indeed reflect the different chemical composition of the *Ph*TAC125 biofilms. For the purpose of a quantitative comparison, the spectra of the biofilms in Fig. 4 were normalized with respect to the amide I band (~ 1665 cm^{-1}). Therefore, the following comparison between the biofilms refers to the relative content of nucleic acids or carbohydrates with respect to the protein content (Henry et al., 2017).

The strongest evidence was the presence of Raman bands at

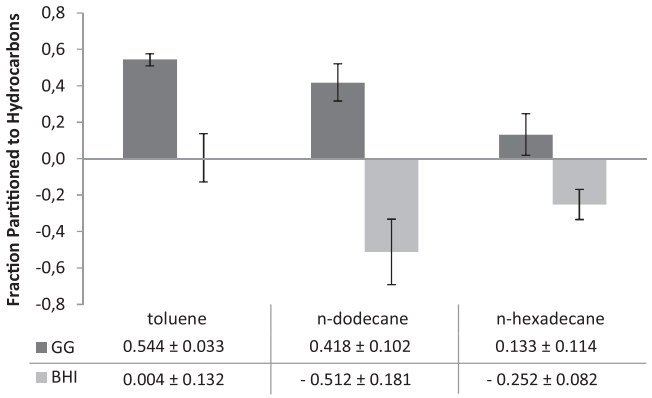

Fig. 2. MATH assay of *Ph*TAC125 A–L biofilms. The fraction of the biofilms partitioned in the hydrocarbon phase measured by means of MATH assay. The bacterial suspensions are contacted with toluene, n-dodecane, and n-hexadecane. The cells were suspended in 200 mM NaCl for all the measurements. Each data point represents the mean ± SD of four independent samples.

Table 1
Motility of *Ph*TAC125 in different conditions. Analysis of the ability of *Ph*TAC125 to swarm into a semi-solid medium. The motility was expressed as the length of the path travelled on the BHI and GG soft-agar plates per unit of time (mm/h). The data are reported as the mean ± SD of three independent experiments.

	MOTILITY (mm/h)	
	0 °C	15 °C
BHI	0.092 ± 0.008	0.375 ± 0.02
GG	0.016 ± 0.002	0.104 ± 0.003

674 cm^{-1} (the guanine–ring mode), 786 cm^{-1} (mostly the DNA phosphodiester backbone mode), and 815 cm^{-1} (mostly the RNA phosphodiester backbone mode) only in the sample grown in the GG medium. These bands, which represent important nucleic acid fingerprints (Carey et al., 2017), were, on the contrary, not detectable in the biofilm obtained in the BHI. Other nucleic acid-related bands can be compared between the two samples, consistently indicating a much higher nucleic acid relative content in the GG-grown biofilms. Indeed, the Raman bands at 1588 cm^{-1} (the adenine/guanine ring) and at 1178 cm^{-1} (the guanine-ring) presented a higher intensity in the latter sample. Moreover, the band at 1488 cm^{-1} (the adenine/guanine ring), after normalization to amide I (1665 cm^{-1}), was ~5 times higher in the GG- than in the BHI- grown biofilms.

The relative content of carbohydrates can be estimated by the ratio I1130/I1007, related to the carbohydrate and Phe-ring bands, respectively (Carey et al., 2017; Henry et al., 2017). Other carbohydrate-related Raman bands were located at 1366 and 1400 cm^{-1}. All these markers consistently indicated a slightly higher carbohydrate/protein content in the biofilms grown in the GG medium compared to those obtained in the BHI medium.

Concerning the analysis of biofilms grown at 15 °C, as a high fluorescence was observed for biofilms grown in both media, a further washing step was carried out to get rid of this interference. Unfortunately, a Raman spectrum of modest quality was collected only for the sample grown in the GG medium (data not shown). Despite its modest quality, the Raman spectrum recorded allowed us to see at least detectable nucleic acid-related Raman bands at 674 cm^{-1}, 786 cm^{-1}, and 815 cm^{-1} with a relative nucleic acid/protein Raman intensity similar to that observed for the biofilms grown at 0 °C, indicating that the specific growth temperature did not influence the relative nucleic/protein ratio.

3.6. Sugar analysis of PhTAC125 biofilms

In order to obtain information on the polysaccharides present in the different *Ph*TAC125 biofilm, samples were analyzed by 14% DOC-PAGE and visualized by using the silver nitrate method (Tsai and Frasch, 1982) (Fig. S2). The silver nitrate showed the presence in all the samples of one band at low molecular masses, corresponding to LPS, the

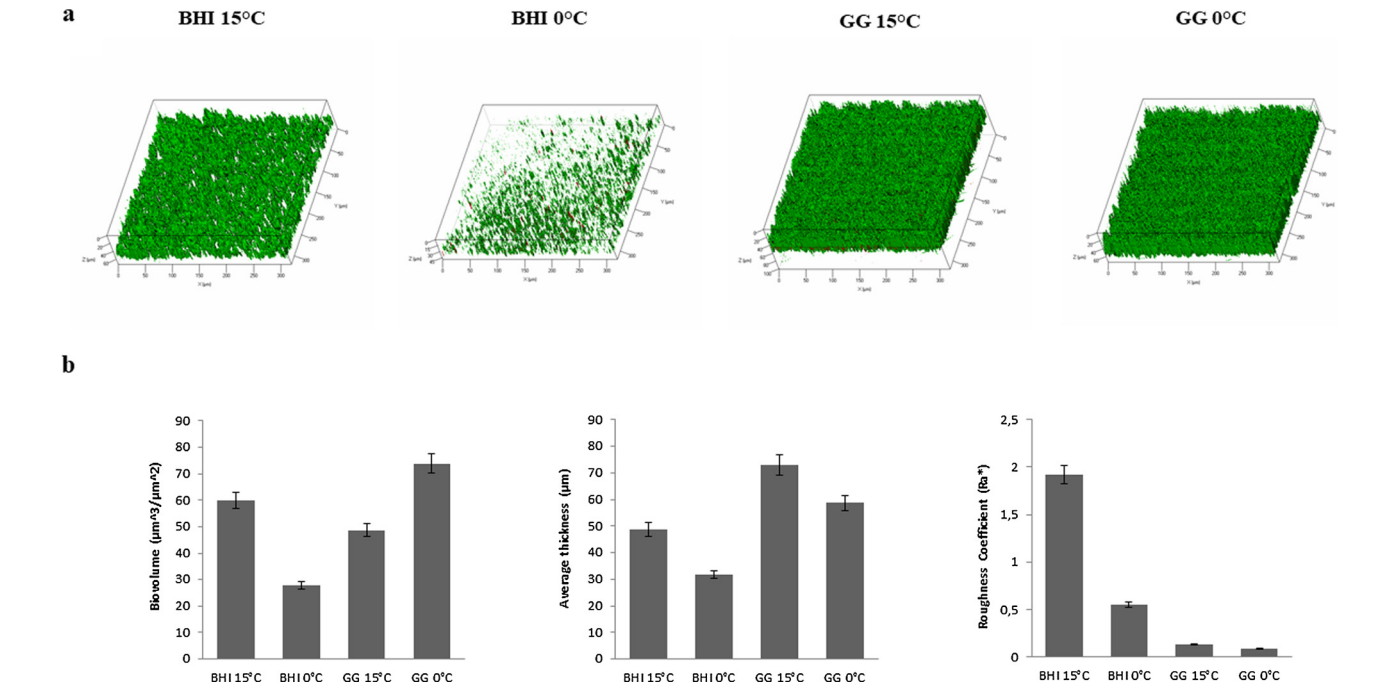

Fig. 3. CLSM analysis of *Ph*TAC125 biofilms. Analysis of the effect of temperature and growth medium on the *Ph*TAC125 biofilm structure. (a) CLSM analysis of *Ph*TAC125 biofilm grown in chamber slides at 15 °C and 0 °C in the BHI medium and GG medium for 24 h. The three-dimensional biofilm structures were obtained using the LIVE/DEAD® Biofilm Viability Kit. (b) COMSTAT quantitative analysis of the biomass, average thickness and roughness coefficient of the *Ph*TAC125 biofilms at all the tested conditions. (For interpretation of the references to colour in the text, the reader is referred to the web version of this article).

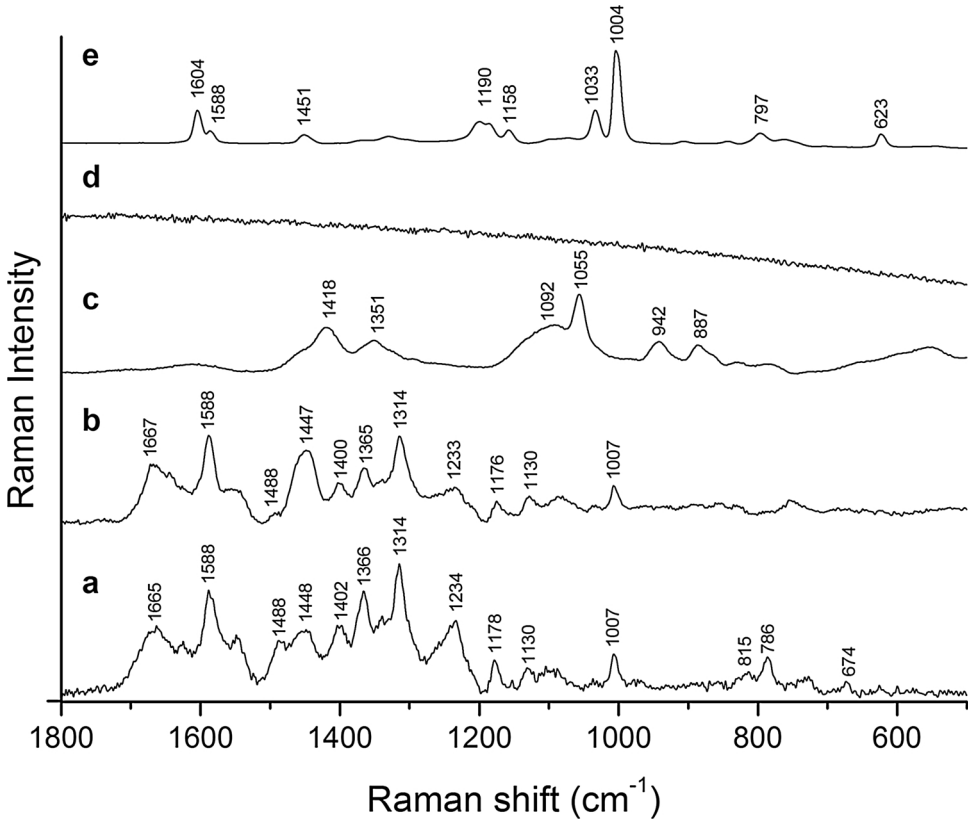

Fig. 4. Raman analysis of *Ph*TAC125 biofilms. Raman spectra (500–1800 cm^{-1}) collected with 514 nm laser, 60 s exposure, and 1 µm spot size: (a) GG-grown biofilm at 0 °C, (b) BHI-grown biofilm at 0 °C, (c) GG medium, (d) BHI medium, and (e) polystyrene substrate. The spectra a and b are normalized with respect to the amide I band (1665 cm^{-1}).

Table 2
Biofilm sugar analysis profile. Monosaccharides percentage calculated for each biofilm growth condition referred to the relative abundance of each component compared to the total sugars.

Carbohydrate	*Ph*TAC125 S-L Biofilm 0 °C GG	*Ph*TAC125 A-L Biofilm 0 °C BHI	*Ph*TAC125 A-L Biofilm 15 °C BHI	*Ph*TAC125 A-L Biofilm 15 °C GG
Ribose	37.6%	3.4%	–	22.5%
Mannose	–	1.1%	1.8%	1.2%
Galactose	13.1%	36.1%	36.2%	15.7%
Glucose	4.9%	5.3%	4.5%	7.4%
GlcN	18.1%	18.2%	19.3%	24.6%
Heptose	22.8%	35%	37.5%	22.7%
NAM	3.5%	0.9%	0.7%	5.9%

structure of which had already been characterized (Michela Corsaro et al., 2001). In addition, samples corresponding to GG-grown biofilm and the BHI-grown biofilm, both developed at 0 °C, showed several bands attributable to nucleic acids (Fig. S2 lanes a and b). Glycosyl analysis performed on the *Ph*TAC125 biofilms confirmed the presence of sugars attributable to the lipopolysaccharide (Michela Corsaro et al., 2001) like galactose, glucosamine, heptose, and traces of mannosamine; indeed, in the biofilm a lot of biomass is constituted by cells. Moreover, N-Acetyl-muramic acid (MurNAc, NAM), ribose and glucose were found (Table 2). The presence of ribose confirmed the occurrence of nucleic acids in the samples.

The presence of cellulose in *Ph*TAC125 biofilm was preliminarily investigated by staining cells, grown on GG or BHI agar plates, with the Calcofluor (Fig. S3). Although it is routinely used for this purpose (Zogaj et al., 2001), Calcofluor is not absolutely specific for cellulose (it is known to bind also β[1–4] and β[1–3]-linked glucosyl polymers). Therefore, to confirm the presence of cellulose, the samples of the *Ph*TAC125 biofilms were treated with a cellulase, an enzyme which has the capability to specifically hydrolyze cellulose, leading to free glucose formation. The released glucose was revealed as acetylated alditol, demonstrating the presence of cellulose in all the tested samples (Fig. S4).

3.7. DNase I and proteinase K effect on biofilm formation in different environmental conditions

The role of proteins and eDNA in the 'initial adhesion' and 'early biofilm formation' steps was studied to collect more information on molecular mechanisms involved in *Ph*TAC125 biofilm formation in the four explored conditions. *Ph*TAC125 was grown in the BHI and GG media at 15 °C and 0 °C in static conditions, in the presence of either DNase I or proteinase K, and a quantification of the formed biofilm was performed by means of crystal violet staining (Fig. 5). The results obtained revealed that the treatment with DNase I did not lead to any reduction in the biofilm development but, interestingly, in the GG at 0 °C the nuclease addition led to an increase in the biofilm biomass. The proteinase K treatment, on the other hand, strongly affected the Antarctic bacterium biofilm formation in the BHI medium, whereas the protease addition did not have a great impact on the biofilm formation in the GG medium (Fig. 5).

4. Discussion

The ability of bacteria to form biofilms in many environments is undoubtedly related to the selective advantage that the surface association offers. As previously reported the Antarctic bacterium *Ph*TAC125 is able to form biofilm at 4 °C in BHI and in GG broths and in these conditions, the biofilm formation generally occurs at the air-liquid interface (Papa et al., 2013; Parrilli et al., 2015).

In this paper, the structural characterization of the biofilm of the Antarctic bacterium *Ph*TAC125, produced in response to different nutrient abundance and temperatures, was investigated. In particular, the capability of *Ph*TAC125 to form biofilm was investigated at 15 °C and 0 °C in BHI and GG media.

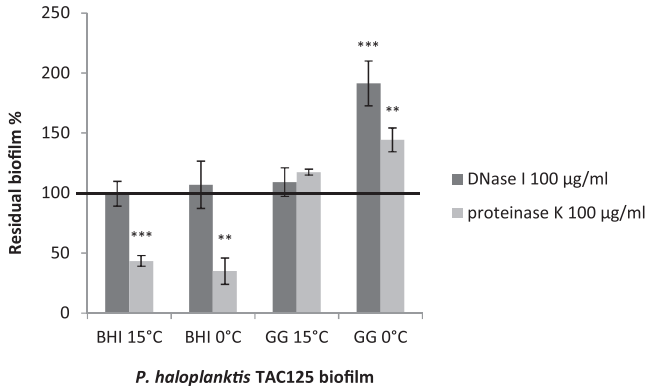

Fig. 5. Analysis of the effect of DNase I and proteinase K on *Ph*TAC125 biofilm formation. The *Ph*TAC125 biofilm formation obtained in the BHI medium or GG medium at 15 °C or 0 °C for 24 h in the absence and presence of DNase I or proteinase K at a concentration of 100 µg/ml. The data are reported as a percentage of the residual biofilm after the treatment. Each data point represents the mean ± the SD of six independent samples; the mean values were compared to the untreated control and considered significant when $p < 0.05$(* $p < 0.05$, ** $p < 0.01$, *** $p < 0.001$) according to the Student t-test.

The Antarctic bacterium resulted to be able to form biofilm and the majority of cells unbudded in the matrix resulted vital (Fig. S1) in all the tested conditions. This result is not surprising since its genomic and metabolic features indicate that this bacterium is adapted to periodic changes in temperature and nutrient availability (Médigue et al., 2005). Data described demonstrating that the cold-adapted bacterium responds to different temperatures (15 °C vs 0 °C) and levels of nutrients abundance (rich medium vs synthetic medium) producing different amount of biofilm, indeed in the synthetic medium, the biofilm quantity was higher than that produced in the rich medium. It's important to underline that in planktonic growth condition the biomass reached in BHI is always higher than that obtained in GG medium (data not shown). Likely, the presence of a lower availability of nutrients could induce a greater production of biofilm since the biofilm matrix can improve the capture of nutrients (Flemming et al., 2016; Shrout et al., 2012; Tolker-Nielsen and Tolker-Nielsen, 2015), and therefore the higher biofilm production could be a strategy to survive in poor nutrient conditions. It's interesting to note that at 0 °C in the GG medium, the bacterium produced biofilm to the same extent as in BHI at 15 °C, indicating that also at low temperatures the energetic cost related to the biofilm production is adequate to the advantages deriving from the biofilm formation. The CLSM analysis on the biofilms produced by *Ph*TAC125 in GG and BHI revealed that the medium composition has a key role also in the definition of the biofilm structure. Actually, the investigation revealed that the biofilm obtained in the GG medium was more compact than the biofilm developed in the rich medium.

It is useful to remark that the temperature and the media composition not only affect the amount and the compactness, but also the typology, of the biofilm. Indeed, the *Ph*TAC125 biofilm accumulates mainly at the air-liquid interface at 15 °C in both BHI and GG media and at 0 °C only in BHI, while, interestingly, it forms biofilm mainly at the solid-liquid interface at 0 °C in the GG medium. Although a correlation between the typology of a biofilm and the growth medium has recently been published (Paytubi et al., 2017), to the best of our knowledge, this is the first report of the effect of the temperature on the typology of biofilm (i.e. in the spatial localization of biofilm). Indeed, the bacterium in GG medium produced a liquid-air biofilm if grown al 15 °C, while in the same medium it produced a biofilm on solid-liquid interface when grown at 0 °C. Anyway, it is remarkable to note that *Ph*TAC125 is able to efficiently produce both submerged biofilms and pellicles and that the *Ph*TAC125 pellicles obtained in the two media resulted to be different. The pellicles obtained in the BHI was slimier and stickier than those obtained in the GG which, in contrast, seemed to be more compact and better structured. Moreover, the *Ph*TAC125 GG pellicles displayed a higher hydrophobicity compared to the *Ph*TAC125 BHI pellicles.

The A–L biofilm formation has been described for various bacteria and proceeds through several stages (Armitano et al., 2013). In the early stages, a thin layer of cells appears at the air-liquid interface (Armitano et al., 2013) and, subsequently, the three-dimensional structures develop as the pellicle grows and thickens (O'Toole et al., 2000). The exact mechanisms underpinning the initial stages of the pellicle formation (i.e. how the cells reach the interface) have not been well-characterized. However, the cell motility seems to strongly influence the A–L biofilm formation, which requires upward swimming capabilities (Kobayashi, 2007). In fact, it has been reported that many bacteria show defects in pellicle formation when the genes involved in the flagellum synthesis are mutated, and, in some species, the ability to form a pellicle is completely abolished (Lemon et al., 2007; Serra et al., 2013). Since several authors have reported that motility might facilitate the bacteria localization near the A–L interface and thereby contribute to the A–L biofilm formation, the different motility of the *Ph*TAC125 cells in the four studied conditions was explored and the bacterium resulted to be slower in the GG than in the BHI medium. This result could explain why the bacterium was unable to form pellicles at 0 °C in the GG medium, but it does not completely clarify why in this condition *Ph*TAC125 was able to form an S-L biofilm. Unpublished proteomic data from our laboratory revealed that the major pilin MshA of type IVa mannose-sensitive hemagglutinin pili is overexpressed when *Ph*TAC125 is grown at 0 °C in a GG medium. Interestingly, type IVa mannose-sensitive hemagglutinin pili are critical for the initial attachment to a surface and for the S-L biofilm formation in several bacteria, such as *Vibrio cholerae* (Watnick et al., 1999) and *Pseudoalteromonas tunicata* (Dalisay et al., 2006). In particular, MshA pili are crucial for the "orbiting" of near-surface motility trajectories (Utada et al., 2014) and it has been demonstrated that when the mannose is added to the medium, in order to saturate the MshA pili binding, the orbiting motility of *V. cholerae* is ablated and the initial surface attachment is impaired (Utada et al., 2014). To assess if the capability of *Ph*TAC125 to form an S-L biofilm in the GG medium at 0 °C was related to the type IV mannose-sensitive hemagglutinin pili, the bacterium was grown in the GG medium at 0 °C in the presence and absence of mannose and the biofilm formation was evaluated (Fig. S5). The presence of mannose reduced the formed biofilm suggesting that, as in *V. cholera*, also in *Ph*TAC125 at 0 °C in the GG medium the surface attachment was mediated by type IV pili and it occurred mainly in these conditions due to the type IV pili overexpression and the reduced motility.

All the data obtained on the biofilm characterization have demonstrated that the specific features like the typology, hydrophobicity, biomass, thickness, and compactness, of *Ph*TAC125 biofilms obtained in different conditions, were deeply different. To assess if these differences might be related to a possible different chemical composition of the biofilm matrix components, the biofilm structures were further investigated by Raman microspectroscopy. This technique has been recently proposed and applied to the chemical characterization of similar biofilms (Carey et al., 2017; Henry et al., 2017; Takahashi et al., 2017). Overall, the Raman investigation of the *Ph*TAC125 biofilms indicated a much higher nucleic acid/protein ratio and an only slightly higher carbohydrate/protein ratio in the biofilms obtained in the GG medium compared to those grown in the BHI medium. The high nucleic acid/protein ratio, reported for the biofilms grown in the GG, could be in accordance with the observation that the *Ph*TAC125 GG pellicles displayed a higher hydrophobicity than the *Ph*TAC125 BHI pellicles. Indeed, several studies have suggested that eDNA increases the hydrophobicity of bacterial cells (Okshevsky and Meyer, 2015). Therefore, it's possible to correlate the hydrophobicity of GG pellicles with a higher content of eDNA, or better with a higher nucleic acid/protein ratio in the biofilm obtained in GG. Moreover, the different nucleic acid/protein relative ratio could also account for the reported

differences in the *Ph*TAC125 biofilm structure (Fig. 3b, roughness coefficient) due to the known influence of eDNA on biofilm three-dimensional architectures (Okshevsky and Meyer, 2015).

Polysaccharides are considered as a significant structural component of the biofilm matrix. As predictable, sugar analysis done on the *Ph*TAC125 biofilms demonstrated the presence of sugars characteristic of the *Ph*TAC125 lipopolysaccharide (Michela Corsaro et al., 2001) like galactose, glucosamine, heptose, and mannosamine. Moreover, N-Acetyl-muramic acid (MurNAc, NAM), ribose and glucose were found. Muramic acid is one of the components of the peptidoglycan structure but also found in LPS structures (Zych et al., 1998; Casillo et al., 2015). As far as we know, it has never been reported as a biofilm component. Instead, ribose has already been found in biofilms (Hung et al., 2005). The presence of glucose in all the samples and the occurrence of a cellulose synthase gene cluster in the *Ph*TAC125 genome (Römling and Galperin, 2015) prompted us to investigate the presence of cellulose in the *Ph*TAC125 biofilm matrix. Cellulose is a significant extracellular matrix component of the biofilms of several ecologically diverse bacteria, and it mediates cell-cell interactions, cell adherence and biofilm formation on biotic and abiotic surfaces (Römling and Galperin, 2015). Four principal types of cellulose synthase operon have been found in various bacterial genomes, in the *Ph*TAC125 genome was found (Römling and Galperin, 2015) an *E. coli*-like type of *bcs* operon which is widespread among the members of beta and gamma subdivisions of proteobacteria, the expression of the cellulose synthase gene cluster is generally stimulated during biofilm formation (Zogaj et al., 2001; Prigent-Combaret et al., 2012). The data reported demonstrated that the cellulose is a constituent of *Ph*TAC125 biofilm matrix in all the tested conditions.

Although the Antarctic bacterium synthesizes cellulose as polysaccharidic component present in the matrix in all the tested conditions, when the different relative content of eDNA and proteins is modulated, it produces biofilm matrices with different characteristics in terms of hydrophobicity, porosity, and roughness.

Last part of the research work was dedicated to assessing if the environmental conditions also influence the *Ph*TAC125 biofilm development process. In particular, the role of proteins and eDNA in the 'initial adhesion' and 'early biofilm formation' steps were studied when the bacterium was grown in the GG or BHI media. The results obtained revealed that the treatment with DNase I did not lead to any reduction in the biofilm development but, interestingly, in the GG at 0 °C the nuclease addition led to an increase in the biofilm biomass. For some bacteria, eDNA, besides its structural role, is required for the initial attachment to surfaces, whereas in other bacteria it plays a role during the transition from the attachment phase to the biofilm maturation phase (Okshevsky et al., 2015). Data reported suggested that the eDNA has a marginal role in the *Ph*TAC125 early biofilm formation both in the GG or BHI. On the other hand, proteins have a key role in Antarctic bacterium biofilm formation in the BHI medium, whereas they did not have a great impact on the biofilm formation in the GG medium. The reported differences in the role of proteins and of eDNA in early biofilm formation steps suggest that the environmental conditions also influence the molecular mechanisms responsible for biofilm establishment and formation.

In conclusion, the capability of *Ph*TAC125 to adopt different biofilm structures in response to changes in its environment appears to be an interesting adaptation strategy and the results herein described give the first hints in biofilm formation in cold environments.

Funding

This research did not receive any specific grant from funding agencies in the public, commercial, or not-for-profit sectors.

Declaration of interest

None.

Appendix A. Supplementary data

Supplementary material related to this article can be found, in the online version, at doi: https://doi.org/10.1016/j.micres.2018.09.010.

References

Allesen-Holm, M., Barken, K.B., Yang, L., Klausen, M., Webb, J.S., Kjelleberg, S., Molin, S., Givskov, M., Tolker-Nielsen, T., 2006. A characterization of DNA release in Pseudomonas aeruginosa cultures and biofilms. Mol. Microbiol. 59, 1114–1128. https://doi.org/10.1111/j.1365-2958.2005.05008.x.

Armitano, J., Méjean, V., Jourlin-Castelli, C., 2013. Aerotaxis governs floating biofilm formation in Shewanella oneidensis. Environ. Microbiol. 15, 3108–3118. https://doi.org/10.1111/1462-2920.12158.

Bester, E., Kroukamp, O., Hausner, M., Edwards, E.A., Wolfaardt, G.M., 2011. Biofilm form and function: carbon availability affects biofilm architecture, metabolic activity and planktonic cell yield. J. Appl. Microbiol. 110, 387–398. https://doi.org/10.1111/j.1365-2672.2010.04894.x.

Carey, P.R., Gibson, B.R., Gibson, J.F., Greenberg, M.E., Heidari-Torkabadi, H., Pusztai-Carey, M., Weaver, S.T., Whitmer, G.R., 2017. Defining molecular details of the chemistry of biofilm formation by Raman microspectroscopy. Biochemistry 56, 2247–2250. https://doi.org/10.1021/acs.biochem.7b00116.

Carillo, S., Pieretti, G., Bedini, E., Parrilli, M., Lanzetta, R., Corsaro, M.M., 2014. Structural investigation of the antagonist LPS from the cyanobacterium *Oscillatoria planktothrix* FP1. Carbohydr. Res. 388, 73–80. https://doi.org/10.1016/j.carres.2013.10.008.

Carillo, S., Casillo, A., Pieretti, G., Parrilli, E., Sannino, F., Bayer-Giraldi, M., Cosconati, S., Novellino, E., Ewert, M., Deming, J.W., Lanzetta, R., Marino, G., Parrilli, M., Randazzo, A., Tutino, M.L., Corsaro, M.M., 2015. A unique capsular polysaccharide structure from the psychrophilic marine bacterium Colwellia psychrerythraea 34H that mimics antifreeze (glyco)proteins. J. Am. Chem. Soc. 137, 179–189. https://doi.org/10.1021/ja5075954.

Casillo, A., Parrilli, E., Filomena, S., Lindner, B., Lanzetta, R., Parrilli, M., Tutino, M.L., Corsaro, M.M., 2015. Structural investigation of the oligosaccharide portion isolated from the lipooligosaccharide of the permafrost psychrophile Psychrobacter arcticus 273-4. Mar. Drugs 13, 4539–4555. https://doi.org/10.3390/md13074539.

Casillo, A., Parrilli, E., Sannino, F., Mitchell, D.E., Gibson, M.I., Marino, G., Lanzetta, R., Parrilli, M., Cosconati, S., Novellino, E., Randazzo, A., Tutino, M.L., Corsaro, M.M., 2017. Structure-activity relationship of the exopolysaccharide from A psychrophilic bacterium: a strategy for cryoprotection. Carbohydr. Polym. 156, 364–371. https://doi.org/10.1016/j.carbpol.2016.09.037.

Christensen, G.D., Simpson, W.A., Younger, J.A., Baddour, L.M., Barrett, F.F., Melton, D.M., Beachey, E.H., 1985. Adherence of coagulase negative Staphylococci to plastic tissue cultures: a quantitative model for the adherence of Staphylococci to medical devices. J. Clin. Microbiol. 22, 996–1006.

Dalisay, D.S., Webb, J.S., Scheffel, A., Svenson, C., James, S., Holmström, C., Egan, S., Kjelleberg, S., 2006. A mannose-sensitive haemagglutinin (MSHA)-like pilus promotes attachment of Pseudoalteromonas tunicata cells to the surface of the green alga Ulva australis. Microbiology 152, 2875–2883. https://doi.org/10.1099/mic.0.29158-0.

De Maayer, P., Anderson, D., Cary, C., Cowan, D.A., 2014. Some like it cold: understanding the survival strategies of psychrophiles. EMBO Rep. 15, 508–517. https://doi.org/10.1002/embr.201338170.

Doghri, I., Rodrigues, S., Bazire, A., Dufour, A., Akbar, D., Sopena, V., Sablé, S., Lanneluc, I., 2015. Marine bacteria from the French Atlantic coast displaying high forming-biofilm abilities and different biofilm 3D architectures. BMC Microbiol. 15, 1–10. https://doi.org/10.1186/s12866-015-0568-4.

Flemming, H.C., Wingender, J., 2010. The biofilm matrix. Nat. Rev. Microbiol. 8, 623–633. https://doi.org/10.1038/nrmicro2415.

Flemming, H.C., Wingender, J., Szewzyk, U., Steinberg, P., Rice, S.A., Kjelleberg, S., 2016. Biofilms: an emergent form of bacterial life. Nat. Rev. Microbiol. 14, 563–575. https://doi.org/10.1038/nrmicro.2016.94.

Fondi, M., Maida, I., Perrin, E., Mellera, A., Mocali, S., Parrilli, E., Tutino, M.L., Liò, P., Fani, R., 2015. Genome-scale metabolic reconstruction and constraint-based modelling of the Antarctic bacterium Pseudoalteromonas haloplanktisTAC125. Environ. Microbiol. 17, 751–766. https://doi.org/10.1111/1462-2920.12513.

Giuliani, M., Parrilli, E., Ferrer, P., Baumann, K., Marino, G., Tutino, M.L., 2011. Process optimization for recombinant protein production in the psychrophilic bacterium Pseudoalteromonas haloplanktis. Process Biochem. 46, 953–959. https://doi.org/10.1016/j.procbio.2011.01.011.

Hall-Stoodley, L., Costerton, J.W., Stoodley, P., 2004. Bacterial biofilms: from the natural environment to infectious diseases. Nat. Rev. Microbiol. 2, 95–108. https://doi.org/10.1038/nrmicro821.

Henry, V.A., Jessop, J.L.P., Peeples, T.L., 2017. Differentiating Pseudomonas sp. strain ADP cells in suspensions and biofilms using Raman spectroscopy and scanning electron microscopy. Anal. Bioanal. Chem. 409, 1441–1449. https://doi.org/10.1007/s00216-016-0077-9.

Heydorn, A., Heydorn, A., Nielsen, A.T., Nielsen, A.T., Hentzer, M., Hentzer, M., 2000.

Quantication of biofilm structures by the novel computer program. Image Process. 2395–2407. https://doi.org/10.1099/00221287-146-10-2395.
Holmström, C., Kjelleberg, S., 1999. Marine Speudoalteromonas species are associated with higter organisms and produce biologically active extracellular agents. FEMS Microb. Ecol. 30, 285–293. https://doi.org/10.1111/j.1574-6941.1999.tb00656.x.
Hung, C.-C., Santschi, P.H., Gillow, J.B., 2005. Isolation and characterization of extracellular polysaccharides produced by Pseudomonas fluorescens Biovar II. Carbohydr. Polym. 61, 141–147. https://doi.org/10.1016/j.carbpol.2005.04.008.
Isnansetyo, A., Kamei, Y., 2003. MC21-A, A bactericidal antibiotic produced by A new marine against methicillin-resistant Staphylococcus aureus. Society 170, 481–490. https://doi.org/10.1128/AAC.47.2.480.
Johnson, T.L., Fong, J.C., Rule, C., Rogers, A., Yildiz, F.H., Sandkvist, M., 2014. The type II secretion system delivers matrix proteins for biofilm formation by vibrio cholerae. J. Bacteriol. 196, 4245–4252. https://doi.org/10.1128/JB.01944-14.
Klein, G.L., Soum-Soutéra, E., Guede, Z., Bazire, A., Compère, C., Dufour, A., 2011. The anti-biofilm activity secreted by a marine Pseudoalteromonas strain. Biofouling 27, 931–940. https://doi.org/10.1080/08927014.2011.611878.
Kobayashi, K., 2007. Bacillus subtilis pellicle formation proceeds through genetically defined morphological changes. J. Bacteriol. 189, 4920–4931. https://doi.org/10.1128/JB.00157-07.
Laemmli, U.K., 1970. Cleavage of structural proteins during the assembly of the head of bacteriophage T4. Nature 227, 680–685. https://doi.org/10.1038/227680a0.
Lemon, K.P., Higgins, D.E., Kolter, R., 2007. Flagellar motility is critical for *Listeria monocytogenes* biofilm formation. J. Bacteriol. 189, 4418–4424. https://doi.org/10.1128/JB.01967-06.
Liao, Y., Williams, T.J., Ye, J., Charlesworth, J., Burns, B.P., Poljak, A., Raftery, M.J., Cavicchioli, R., 2016. Morphological and proteomic analysis of biofilms from the Antarctic archaeon, Halorubrum lacusprofundi. Sci. Rep. 6, 1–17. https://doi.org/10.1038/srep37454.
Liu, X., Beyhan, S., Lim, B., Linington, R.G., Yildiz, F.H., 2010. Identification and characterization of a phosphodiesterase that inversely regulates motility and biofilm formation in Vibrio cholerae. J. Bacteriol. 192, 4541–4552. https://doi.org/10.1128/JB.00209-10.
Margesin, R., Feller, G., 2010. Biotechnological applications of psychrophiles. Environ. Technol. 31, 835–844. https://doi.org/10.1080/09593331003663328.
Médigue, C., Krin, E., Pascal, G., Barbe, V., Bernsel, A., Bertin, P.N., Cheung, F., Cruveiller, S., D'Amico, S., Duilio, A., Fang, G., Feller, G., Ho, C., Mangenot, S., Marino, G., Nilsson, J., Parrilli, E., Rocha, E.P.C., Rouy, Z., Sekowska, A., Tutino, M.L., Vallenet, D., Von Heijne, G., Danchin, A., 2005. Coping with cold: the genome of the versatile marine Antarctica bacterium Pseudoalteromonas haloplanktis TAC125. Genome Res. 15, 1325–1335. https://doi.org/10.1101/gr.4126905.
Michela Corsaro, M., Lanzetta, R., Parrilli, E., Parrilli, M., Luisa Tutino, M., 2001. Structural investigation on the lipooligosaccharide fraction of psychrophilic pseudoalteromonas haloplanktis TAC 125 bacterium. Eur. J. Biochem. 268, 5092–5097. https://doi.org/10.1046/j.0014-2956.2001.02429.x.
O'Toole, G., Kaplan, H., Kolter, R., 2000. Biofilm formation as microbial developmeant. Annu. Rev. Microbiol. 54, 49–79.
Okshevsky, M., Meyer, R.L., 2015. The role of extracellular DNA in the establishment, maintenance and perpetuation of bacterial biofilms. Crit. Rev. Microbiol. 41, 341–352. https://doi.org/10.3109/1040841X.2013.841639.
Okshevsky, M., Regina, V.R., Meyer, R.L., 2015. Extracellular DNA as a target for biofilm control. Curr. Opin. Biotechnol. 33, 73–80. https://doi.org/10.1016/j.copbio.2014.12.002.
Papa, R., Parrilli, E., Sannino, F., Barbato, G., Tutino, M.L., Artini, M., Selan, L., 2013. Anti-biofilm activity of the Antarctic marine bacterium Pseudoalteromonas haloplanktis TAC125. Res. Microbiol. 164, 450–456. https://doi.org/10.1016/j.resmic.2013.01.010.
Parrilli, E., Papa, R., Carillo, S., Tilotta, M., Casillo, A., Sannino, F., Cellini, A., Artini, M., Selan, L., Corsaro, M.M., Tutino, M.L., 2015. Anti-biofilm activity of pseudoalteromonas haloplanktis tac125 against staphylococcus epidermidis biofilm: evidence of a signal molecule involvement? Int. J. Immunopathol. Pharmacol. 28, 104–113. https://doi.org/10.1177/0394632015572751.
Paytubi, S., Cansado, C., Madrid, C., Balsalobre, C., 2017. Nutrient composition promotes switching between pellicle and bottom biofilm in Salmonella. Front. Microbiol. 8. https://doi.org/10.3389/fmicb.2017.02160.
Pieretti, G., Carillo, S., Lindner, B., Lanzetta, R., Parrilli, M., Jimenez, N., Regué, M., Tomás, J.M., Corsaro, M.M., 2010. The complete structure of the core of the LPS from Plesiomonas shigelloides 302-73 and the identification of its O-antigen biological repeating unit. Carbohydr. Res. 345, 2523–2528. https://doi.org/10.1016/j.carres.2010.09.007.
Piette, F., D'Amico, S., Mazzucchelli, G., Danchin, A., Leprince, P., Feller, G., 2011. Life in the cold: a proteomic study of cold-repressed proteins in the antarctic bacterium Pseudoalteromonas haloplanktis TAC125. Appl. Environ. Microbiol. 77, 3881–3883. https://doi.org/10.1128/AEM.02757-10.
Prigent-Combaret, C., Zghidi-Abouzid, O., Effantin, G., Lejeune, P., Reverchon, S., Nasser, W., 2012. The nucleoid-associated protein Fis directly modulates the synthesis of cellulose, an essential component of pellicle-biofilms in the phytopathogenic bacterium Dickeya dadantii. Mol. Microbiol. 86, 172–186. https://doi.org/10.1111/j.1365-2958.2012.08182.x.
Römling, U., Galperin, M.Y., 2015. BacterDial cellulose biosynthesis: diversity of operons, subunits, products, and functions. Trends Microbiol. 23 (9), 545–557. https://doi.org/10.1038/ncomms5913.
Rosenberg, M., Gutnick, D., Rosenberg, E., 1980. Adherence of bacteria to hydrocarbons: a simple method for measuring cell-surface hydrophobicity. FEMS Microbiol. Lett. 9, 29–33. https://doi.org/10.1111/j.1574-6968.1980.tb05599.x.
Sannino, F., Giuliani, M., Salvatore, U., Apuzzo, G.A., de Pascale, D., Fani, R., Fondi, M., Marino, G., Tutino, M.L., Parrilli, E., 2017. A novel synthetic medium and expression system for subzero growth and recombinant protein production in Pseudoalteromonas haloplanktis TAC125. Appl. Microbiol. Biotechnol. 101, 725–734. https://doi.org/10.1007/s00253-016-7942-5.
Sauer, K., Camper, A.K., Ehrlich, G.D., Costerton, J.W., Davies, D.G., 2002. Pseudomonas aeruginosa. J. Bacteriol. 184, 1140–1154. https://doi.org/10.1128/JB.184.4.1140.
Saville, R.M., Rakshe, S., Haagensen, J.A.J., Shukla, S., Spormann, A.M., 2011. Energy-dependent stability of Shewanella oneidensis MR-1 biofilms. J. Bacteriol. 193, 3257–3264. https://doi.org/10.1128/JB.00251-11.
Seper, A., Fengler, V.H.I., Roier, S., Wolinski, H., Kohlwein, S.D., Bishop, A.L., Camilli, A., Reidl, J., Schild, S., 2011. Extracellular nucleases and extracellular DNA play important roles in Vibrio cholerae biofilm formation. Mol. Microbiol. 82, 1015–1037. https://doi.org/10.1111/j.1365-2958.2011.07867.x.
Serra, D.O., Richter, A.M., Klauck, G., Mika, F., Hengge, R., 2013. Microanatomy at cellular resolution and spatial order of physiological differentiation in a bacterial biofilm. MBio 4. https://doi.org/10.1128/mBio.00103-13.
Shrout, J.D., Chopp, D.L., Just, C.L., Hentzer, M., Givskov, M., Parsek, M.R., 2006. The impact of quorum sensing and swarming motility on Pseudomonas aeruginosa biofilm formation is nutritionally conditional. Mol. Microbiol. 62, 1264–1277. https://doi.org/10.1111/j.1365-2958.2006.05421.x.
Shrout, J.D., Tolker-Nielsen, T., Givskov, M., Parsek, M.R., 2012. The contribution of cell-cell signalling and motility to bacterial biofilm formation. MRS Bull. 36, 367–373. https://doi.org/10.1557/mrs.2011.67.
Smith, H.J., Schmit, A., Foster, R., Littman, S., Kuypers, M.M.M., Foreman, C.M., 2016. Biofilms on glacial surfaces: hotspots for biological activity. npj Biofilms Microbiomes 2. https://doi.org/10.1038/npjbiofilms.2016.8.
Takahashi, C., Ueno, K., Aoyama, J., Adachi, M., Yamamoto, H., 2017. Imaging of intracellular behavior of polymeric nanoparticles in Staphylococcus epidermidis biofilms by slit-scanning confocal Raman microscopy and scanning electron microscopy with energy-dispersive X-ray spectroscopy. Mater. Sci. Eng. C 76, 1066–1074. https://doi.org/10.1016/j.msec.2017.03.132.
Tolker-Nielsen, T., Tolker-Nielsen, Tim, 2015. Biofilm development. Microbiol. Spectr. 3, 1–12. https://doi.org/10.1128/microbiolspec.
Toyofuku, M., Inaba, T., Kiyokawa, T., Obana, N., Yawata, Y., Nomura, N., 2016. Environmental factors that shape biofilm formation. Biosci. Biotechnol. Biochem. 80, 7–12. https://doi.org/10.1080/09168451.2015.1058701.
Tsai, C.M., Frasch, C.E., 1982. A sensitive silver stain for detecting lipopolysaccharides in polyacrylamide gels. Anal. Biochem. 119, 115–119. https://doi.org/10.1016/0003-2697(82)90673-X.
Utada, A.S., Bennett, R.R., Fong, J.C.N., Gibiansky, M.L., Yildiz, F.H., Golestanian, R., Wong, G.C.L., 2014. Vibrio cholerae use pili and flagella synergistically to effect motility switching and conditional surface attachment. Nat. Commun. 5. https://doi.org/10.1038/ncomms5913.
Vergara, A., Lorber, B., Sauter, C., Giegé, R., Zagari, A., 2005. Lessons from crystals grown in the advanced protein crystallisation facility for conventional crystallisation applied to structural biology. Biophys. Chem. 118 (2–3), 102–112. https://doi.org/10.1016/j.bpc.2005.06.014.
Vergara, A., Russo Krauss, I., Montesarchio, D., Paduano, L., Merlino, A., 2013. Investigating the ruthenium metalation of proteins: X-ray structure and Raman microspectroscopy of the complex between RNase A and AziRu. Inorg. Chem. 52, 10714–10716. https://doi.org/10.1021/ic401494v.
Watnick, P.I., Fullner, K.J., Kolter, R., 1999. A role for the mannose-sensitive hemagglutinin in biofilm formation by Vibrio cholerae El Tor. J. Bacteriol. 181, 3606–3609.
Whitchurch, C.B., Tolker-Nielsen, T., Ragas, P.C., Mattick, J.S., 2002. Extracellular DNA required for bacterial biofilm formation. Science 295, 1487. https://doi.org/10.1126/science.295.5559.1487.
Wilmes, B., Hartung, A., Lalk, M., Liebeke, M., Schweder, T., Neubauer, P., 2010. Fed-batch process for the psychrotolerant marine bacterium Pseudoalteromonas haloplanktis. Microb. Cell Fact. 9, 1–9. https://doi.org/10.1186/1475-2859-9-72.
Wimpenny, J., Manz, W., Szewzyk, U., 2000. Heterogeneity in biofilms. FEMS Microbiol. Rev. 24 (5), 661–671. https://doi.org/10.1016/S0168-6445(00)00052-8.
Yildiz, F., Fong, J., Sadovskaya, I., Grard, T., Vinogradov, E., 2014. Structural characterization of the extracellular polysaccharide from Vibrio cholerae O1 El-Tor. PLoS One 9. https://doi.org/10.1371/journal.pone.0086751.
Zogaj, X., Nimtz, M., Rohde, M., Bokranz, W., Römling, U., 2001. The multicellular morphotypes of *Salmonella typhimurium* and *Escherichia coli* produce cellulose as the second component of the extracellular matrix. Mol. Microbiol. 39, 1452–1463. https://doi.org/10.1046/j.1365-2958.2001.02337.x.
Zych, K., Knirel, Y.A., Paramonov, N.A., Vinogradov, E.V., Arbatsky, N.P., Senchenkova, S.N., Shashkov, A.S., Sidorczyk, Z., 1998. Structure of the O-specific polysaccharide of Proteus penneri strain 41 from a new proposed serogroup O62. FEMS Immunol. Med. Microbiol. 21, 1–9. https://doi.org/10.1016/S0928-8244(98)00012-1.